**WOOD RESEARCH** doi.org/10.37763/wr.1336-4561/67.3.423436
**e-ISSN 2729-8906**
**67(3): 2022 423-436 pp.**

# MODELLING OF STEEL TO TIMBER JOINT EXPOSED TO FIRE

KRISTÝNA VOPATOVÁ, KAMILA CÁBOVÁ
CZECH TECHNICAL UNIVERSITY IN PRAGUE
CZECH REPUBLIC

(RECEIVED NOVEMBER 2021)

## ABSTRACT

The paper presents an investigation on a timber joint with an inserted steel plate under fire exposure. According to standard EN 1995-1-2 (2004), the fire resistance of unprotected timber joints is limited to 30 min. However, several studies have shown that these joints can achieve higher fire resistance comparing to values given in the standard. In order to verify this, a numerical model of bolted steel-timber joint at elevated temperature was created. The presented model is focused on heat transport in the joint, which is affected by the presence of the steel plate and bolts. The model was validated on experimental results taken from literature and on measurement from a fire tests conducted in a medium-sized furnace. Considering the results of validation, the model has a good ability to predict residual cross-section, temperature of steel plate and bolts and temperature of timber elements. The results of validated numerical model are also compared to the analytical model.

KEYWORDS: Timber joint, steel plate, fire test, numerical model, validation.

## INTRODUCTION

Within timber structures, it is popular to design joints with inserted steel plates, which are able to withstand higher loads. These joints are called “steel-timber” joints according to the EN 1995-1-1 (2004). To design safe structures, reliable data based on analytical models, numerical models or a combination of both are necessary. One of the most important sources of reliable data are experimentally validated numerical models (Cábová et al. 2019). Numerical models are usually based on the finite element method (FEM). Analytical solution of joints may be solved by component method. The component method is commonly used for design at normal temperatures, but studies such as Simões da Silva et al. (2001) extended the use of this method to predict the behaviour of joints of steel structures at elevated temperatures. During modelling at

elevated temperatures, it is necessary to define a number of simplifications due to the complexity of joint behaviour, especially for timber elements.

Many studies have looked at the load-bearing capacity of steel-timber joints at normal temperatures (Hassanieh, 2017, Johansen 1949, Kharouf et al. 2003, Xu et al. 2009, Schmidt and Kaliske 2009). Palma et al. (2014) and Palma and Frangi (2019) investigated the effect of joint geometry especially the spacing of fasteners during the fire. The test results showed a significant dependence of the fire resistance of the designed joints on the width of the lateral elements. As the width of the lateral elements increased, the fire resistance also increased. Increasing the thickness of the side elements leads to higher fire resistance and it is also more effective than increasing the height.

Frangi et al. (2009) conducted an extensive experimental study focusing on beam-column connections under normal temperature and fire conditions. This involved loading perpendicular to the grain of the timber. Subsequently, they developed a numerical model to correctly simulate the deformation and temperature histories. The specimens were simultaneously loaded with a constant tensile load corresponding to 30% of the load capacity under normal temperature during the fire tests. Aspects such as larger beam-to-column spacing, reduced fastener spacing and self-tapping bolt design have a negative effect on fire resistance.

Another studies focused on fire resistance of steel-timber joints (Audebert et al. 2011, 2012) investigated the influence of the fasteners used. Pin connections with one bolt in each row of fasteners were proposed. From the data, the effect of the stud on the load carrying capacity was demonstrated. From the measured data, an empirical function of the dependence of the fire resistance time on the diameter of the fastener, the thickness of the lateral member and the reduction factor of the load effect in a fire situation was derived.

This work is a part of a research which aims to present an accurate approach in modelling of bolted steel-timber joints under tensile stress at elevated temperature. For this purpose, the numerical model was created, the model was validated on fire experiments, and the results of validated numerical model were compared to the analytical model. Some preliminary results of analytical models and experimental work have been presented in Vopatová et al. (2019, 2021a,b), but no numerical model and no proper validation to experiments has been provided. Detailed data of experiments may be found in Zeman (2021).

## MATERIAL AND METHODS

### Joint configuration

For the purpose of this research the bolted steel-timber joint configuration presented in Fig. 1 has been designed in respect to EN 1995-1-1 (2004). The timber element has a square cross-section with dimensions 140 x 140 mm. The steel plate is located in the middle of the timber elements, and it is 300 mm long, 6 mm thick, and 80 mm wide. Four M10 bolts are used on each side of each timber element. Bolt spacing as well as other details related to measurement during fire experiments are shown in Fig. 1. The designed bolted steel-timber joint is smaller than conventional bolted steel-timber joints. This fact is due to the limitation caused by

the experimental equipment, mainly the furnace. However, the designed joint is still usable in practice.

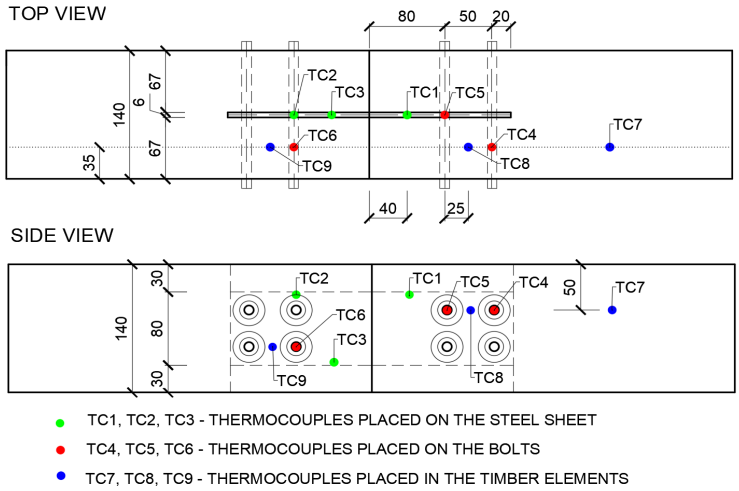


*Fig. 1: The sample layout with thermocouple placement.*

Grown timber of strength class C24 is used for timber elements of the joint (EN 338, 2016). The inserted steel plate is made of S235 steel class without surface treatment. Holes drilled into the elements are of the same dimension as bolts. The M10 bolts were made of threaded rods. The bolt is held by an 8 mm high nut on each end of a threaded rod. Between nuts and timber elements, construction washers with a diameter of 30 mm and a height of 2.5 mm are used. The threaded rods, nuts, and washers are also without surface treatment. The connection is designed to meet fire resistance R30 according to EN 1995-1-2 (2004). The fire resistance is achieved by increased thickness ($a_{fi}$ = 18 mm). The ends of bolts with nuts are left uncovered, protruding out of the timber element.

**Analytical model**

The analytical model is based on the calculation of load-bearing capacity at normal temperatures according to EN 1995-1-1 (2004) and load-bearing capacity at elevated temperatures according to EN 1991-1-2 (2004).

At normal temperatures, according to EN 1995-1-1 (2004), three possible modes of failure are used to calculate the load-bearing capacity of the bolted joint. The first mode of failure (F failure mode) is caused by pushing the bolt into the timber element (Fig. 2a). In the second case (G failure mode) a failure occurs due to the pressure of the bolt on the timber element and the simultaneous formation of a plastic bolt deformation in place of the inserted steel plate (Fig. 2a). In the third failure mode (H failure mode) plastic deformations form on the bolt in place of the inserted steel plate and also in the area of the timber element (Fig. 2a).

At elevated temperatures, the load-bearing capacity of the weakened steel plate may influence the resulting load-bearing capacity.

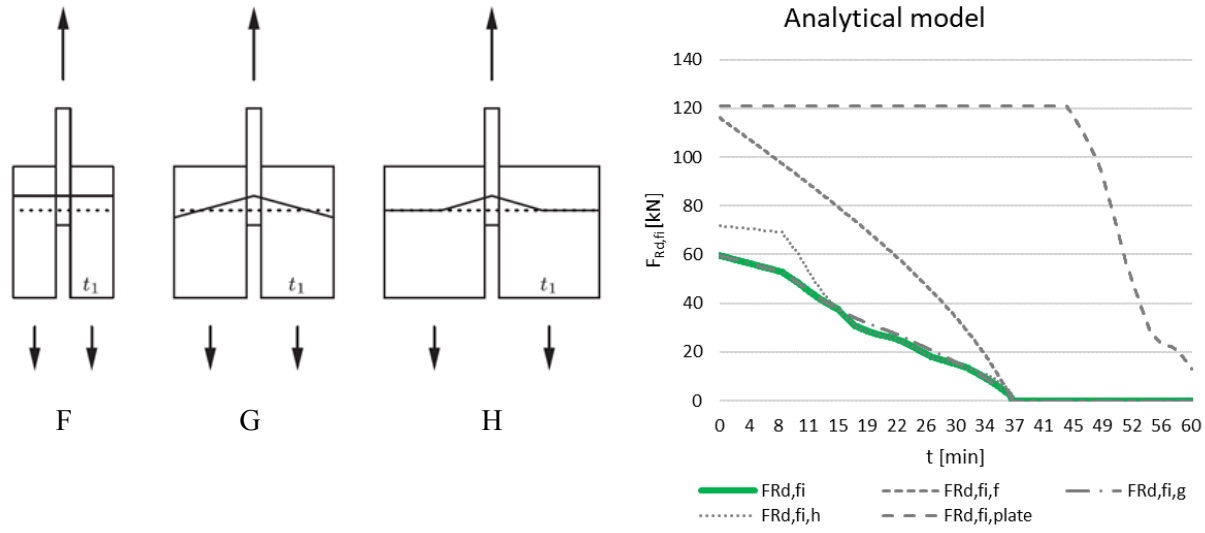


a) b)

*Fig. 2: a) Failure modes of steel-to-timber connections; b) Load-bearing capacities for failure modes, the steel plate, and the assembled load-bearing capacity.*

The analytical model is applied to calculate the load-bearing capacity of the steel-timber joint described in the previous chapter with corresponding dimensions and geometry. The fire exposure following the standard temperature curve according to EN 1991-1-2 (2004) is considered. Material characteristics such as the yield strength of the bolt and the yield strength of the inserted steel plate are reduced in the analytical model. At the same time, the dimensions and material characteristics of timber elements are also reduced with respect to elevated temperatures. The assembled load-bearing capacity based on the failure modes described above as the function of the time of the fire is shown in Fig. 2b. Load-bearing capacities for F, G, and H failure modes are also shown in Fig. 2. Moreover, the figure also depicts the load-bearing capacity of the inserted steel plate.

The resulting load-bearing capacity is then the minimum value of the four individual load-bearing capacities. It can be seen from the graph in Fig. 2b that the assembled load-bearing capacity is mainly affected by the g-mode within the first 15 min. After 15 min, the assembled load-bearing capacity is mainly given by the H failure mode. All three modes of failure (F, G, and H failure modes) fall down to zero at 37 min. According to the analytical model, the inserted plate does not lose its load-bearing capacity for 45 min.

**Experimental study**

In order to measure temperatures in various places of the joint, two specimens of steel-timber joint described above were prepared for testing under fire exposure in a furnace. Temperatures measured served for better understanding of ongoing processes in the joint during fire exposure, but mainly the temperatures were used for validation of a numerical model presented in the next chapter.

**Test setup**

In order to investigate the temperature distribution and its transport into individual components of the joint during the fire, nine thermocouples of the K-type were inserted into the specimens. The placements of all nine thermocouples, as well as the main dimensions of the tested steel-timber joint, are presented in Fig. 1. Three thermocouples (TC1-3) were located on the steel sheet, three thermocouples (TC4-6) were located on the bolts in the depths of 35 mm and 70 mm within the timber element, and three more thermocouples (TC6-9) were placed in the timber elements in the depth of 35 mm.

The fire tests were carried out in a MiniFUR furnace in the UCEEB laboratory. The MiniFUR is used for indicative medium-sized tests. In Fig. 3 the geometry and dimensions of the MiniFUR furnace are shown. In the upper half of the furnace, it is possible to achieve a temperature close to the standard temperature curve.

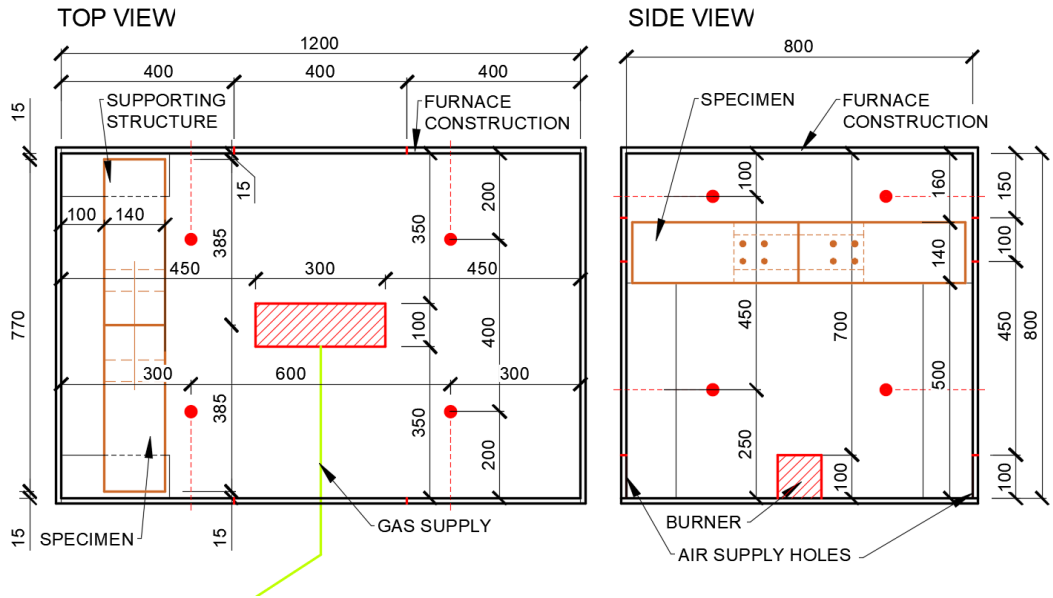


*Fig. 3: MiniFUR furnace with the location of a specimen.*

In the furnace propane gas was used as a fuel. The control system regulates the propane gas inflow and ventilation output to achieve the temperature following the standard temperature curve. However, during the experiments with timber, there is an extra heat caused by burning of timber. Therefore, a reference experiment with one steel-timber joint specimen inside the furnace was conducted. During the reference test the control system was set to a basic curve setup corresponding to standard temperature curve. From the reference test, it was measured that the burning of timber element does not change the furnace environment significantly. The only temperatures that changed due to burning of timber were the temperatures close to the timber element Therefore, there was no need to correct the control system due to extra heat coming from burning of timber.

After the reference experiment, two regular experiments with bolted steel-timber joint were carried out. During the experiments, all the furnace constraints for specimen placement were respected in order to achieve optimal gas flow and, consequently, optimal test results.

At the beginning of each test, the exhaust ventilation output was set to 30%, which increased to 50-60% in the later phase of the experiment.

Each experiment was terminated after 30 min. Then, the sample was taken out of the furnace and cooled down in the water. Fig. 4 shows specimen 1 before cooling down in the water. Afterward, the specimens were measured, and all the results were compared with the analytical and numerical model.

*Fig. 4: Specimen 1 before taking out of the furnace and cooling down in the water.*

**Numerical study**

Using finite element ANSYS 19.R3 software (ANSYS Theory Reference 1999, ANSYS Workbench documentation 2005), a numerical model of bolted steel-timber joint under a fire load was developed. To simulate joint behaviour, a number of simplifications was introduced. Despite the simplifications, the developed numerical model was successfully validated on experiments.

**Geometry, input values, and material properties**

For the purpose of numerical study, the joint of the same geometry as the bolted steel-timber joint shown on Fig. 1 was modelled. The model is presented in Fig. 5. To optimize the computational time, the axis of symmetry is used. A tetrahedral computing mesh was used in this model. The size of the mesh is set for each object differently to optimize computational time without affecting the resulting values. The thermal load was applied with following constants: a single convective heat transfer coefficient $\alpha_c = 25$ $W \cdot m^{-2} K^{-1}$, emissivity of steel elements without surface treatment $\varepsilon_{m,s} = 0,7$ according to EN 1993-1-2 (2005), and emissivity of timber elements $\varepsilon_{m,t} = 0,94$. Temperature profiles measured on thermocouples on the opposite side of the furnace at sample level were applied as a thermal load in the numerical model. The bulk density was set to depend on the temperature according to EC5.

A number of simplifications have been made, such as a simplified shape of a threaded rod and nut (Fig. 5). The threaded rods are cylinders with a diameter of 10 mm, and the nuts are modelled as cylinders with a diameter of 17 mm. The threaded rod protrudes 3 mm above

the nut. To eliminate duplication of thermal loads, the timber element is divided into three volumes. The first volume is under the bolt head, the second volume is the main body of the timber element exposed to thermal loads, and the third volume is a 3 mm layer next to the steel sheet.

To include the effect of steel sheet embedding into temperature development, an air gap is modelled above the inserted steel plate with the default air settings. This air gap can be seen in Fig. 5 together with all three volumes of the timber element as well as the steel sheet, bolts, nuts, and washers.

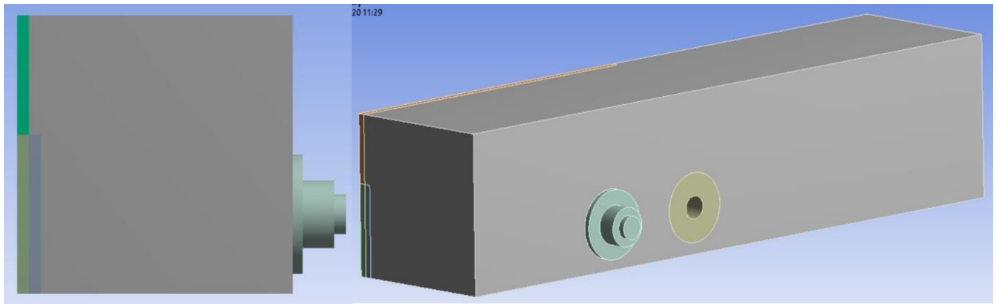

a) b)

*Fig. 5: The visualization of numerical model: a) side view; b) axonometry.*

Material properties of timber were drawn from several literature sources, including EN 1995-1-2 (2006) and Janssens (1994). In the third timber volume, a layer of 3 mm thick close to the steel sheet with modified material properties of timber was introduced. The modification lies in change of specific heat capacity of timber, as recommended in (Audebert 2014). This modification was done in order to take into account the effect of accumulated water vapor thanks to the barrier formed by the sheet.

The model has a few limitations. It does not take into account the transport of water vapour, the release of bound water and the subsequent condensation of the sheet. It only takes into account the material properties depending on the temperature and accumulated water vapour and their condensation at the sheet by modifying of the specific heat capacity of wood in a thickness of 3 mm at the steel plate.

**Model validation**

In order to achieve high reliability, two-step validation was performed. In the first step, the numerical model was validated using experimental results from Audebert et al. (2011), and in the second step, the numerical model was validated on result of performed experiments described above. A numerical model with the same joint geometry as in work by Audebert et al. (2011) was created. The timber used in the referred experiments was GL28h with a density of 450 $kg \cdot m^{-3}$. A thermal load following the ISO834-1 (1999) temperature curve was used. Four different versions of the model were created with four different sets of material properties. Based on results of this validation it was shown that the model results correspond to the referred experiments when material properties introduced by Janssens (1994) and adjusted specific heat

capacity in modified timber layer close to the steel sheet according to Audebert et al. (2014) are implemented in the model.

Afterward, a numerical model of own bolted steel-timber joint shown in Fig. 1 was created. Input parameters of the model according to material properties of Janssens with adjustment of specific heat capacity of modified timber layer were used. The main difference in material properties referred by Janssens (1994) and the own bolted steel-timber joint was the density of C24 class timber equal to 410 $kg \cdot m^{-3}$.

## RESULTS AND DISCUSSION

### The residual cross-section

Tab. 1 compares the thicknesses of the carbonized layer calculated from the analytical model, numerical model, and experimentally measured values. According to the analytical model, the thickness of the carbonized layer is 24 mm after 30 min of fire, considering a constant burning rate, and the thickness of the residual cross-section $t_1$ is 43 mm after 30 min of fire. The residual cross-sections (outside the steel elements, at the steel sheet position and at the bolt position) of a timber sample after fire are shown in Fig. 6. The measured thickness $t_1$ of the residual cross-section of the sample after the test was equal to 38 mm outside the bolt and 32 mm at the bolt position. In the numerical model, a 300°C isotherm was considered as the boundary between carbonized layer and the residual cross-section. From this numerical model, the thickness of the residual cross-section was calculated to be 35 mm. In the cross-section at the bolt position, the temperature is higher than 300°C after 20 min of fire; therefore, the whole cross-section is considered to be carbonized.

*Tab. 1: Carbonized layer after 30 min fire.*

| Source | Place of measurement | Carbonized layer (mm) | Residual thickness $t_1$ (mm) |
|---|---|---|---|
| Analytical model | | 24 | 43 |
| Numerical model | Between the bolts | 32 | 35 |
| Experiment | Between the bolts | 29 | 38 |
| | In place of the bolt | 35 | 32 |

*Fig. 6: The timber elements after the fire test.*

### Temperatures on steel elements

The development of temperatures on bolts calculated by the aid of the analytical model using the incremental method corresponds to the course of the maximum temperature in the bolt

calculated by the numerical model (Fig. 7). These maximum temperatures occur on the surface of the bolt, which is exposed to thermal load, in the model. The temperature measured in the centre of a bolt during the fire test, i.e. in the axis of the model symmetry of the joint, is half the temperature measured on the surface of the bolt. The results of temperatures in the centre (in Fig. 7 denoted as bolts MIN) and on the surface of the bolt (denoted as bolts MAX) calculated by the aid of the numerical model correspond well with the temperatures measured during the fire test.

Temperatures measured at the depth of 35 mm during the fire test are in good agreement with temperatures calculated in the same depth in the numerical model. Looking at the maximal values of temperature in the depth of 35 mm, measured temperature and calculated one in the numerical model are about 300°C lower than the temperatures derived from the analytical model. The analytical model gives conservative values of temperatures on the bolt.

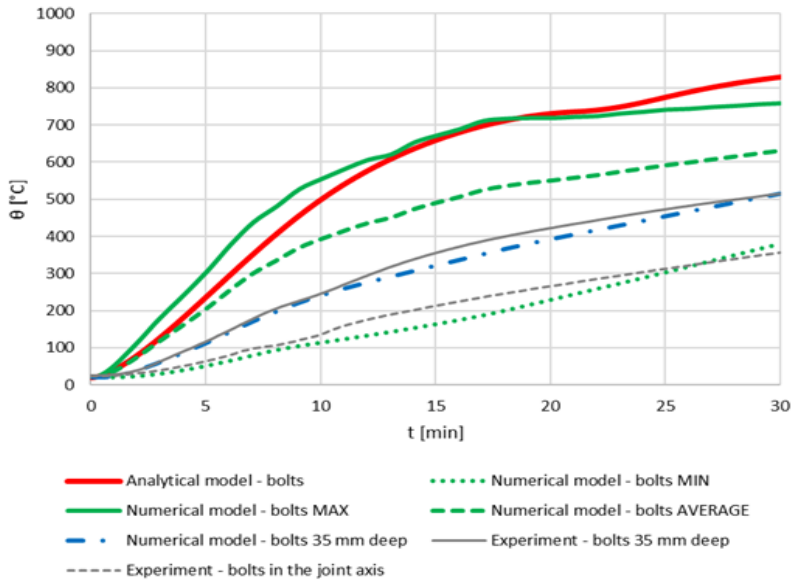


*Fig. 7: Comparison of bolt temperatures.*

The temperatures on the steel sheet coming from the analytical model in time of 30 min are about 180°C lower than the corresponding temperatures in the weakened section of the sheet obtained from the experiment and the numerical model (Fig. 8). Calculation of the steel sheet temperature in the analytical model is based on the incremental method. According to it, the temperature of the steel on the exposed surface is calculated. The temperatures on the sheet surface according to the numerical model (numerical model sheet MIN) are comparable to the temperatures of the analytical model. The analytical model does not take into account the temperature increment from the bolt. Although the temperatures at the weakened point are actually higher, this does not have a large effect on the overall load capacity. Only the load-bearing capacity of the sheet will then approach the total load-bearing capacity from the combination of individual failure states.

**Temperature on timber elements**

Temperature was also measured in the wooden elements using TC7, TC8 and TC9 thermocouples. The temperatures measured by thermocouple TC7, which was placed in a volume of the wood not affected by the elevated temperature of the steel elements, are shown in Fig. 9. Thermocouples TC8 and TC9 were placed between the bolts and therefore the resulting temperatures in the wood were affected by elevated temperatures in the steel components, see Figs. 10 and 11, and they are higher comparing to TC7. The numerical model in ANSYS software does not take into account the chemical reactions during wood burning causing the temperature increase. The model only reflects temperature dependent material properties taken from EN 1995-1-2 (2006) and Janssens (1994). In Figs 9, 10 and 11 temperatures calculated with both material properties are denoted as J for Janssens properties and EN for Eurocode properties. The results of temperatures calculated at the positions of all three thermocouples show that numerical model including material properties recommended by Janssens (1994) fits the measured temperatures better. Similarly to results presented in Audebert et al. (2014), the experimental data grow faster comparing to numerically calculated values.

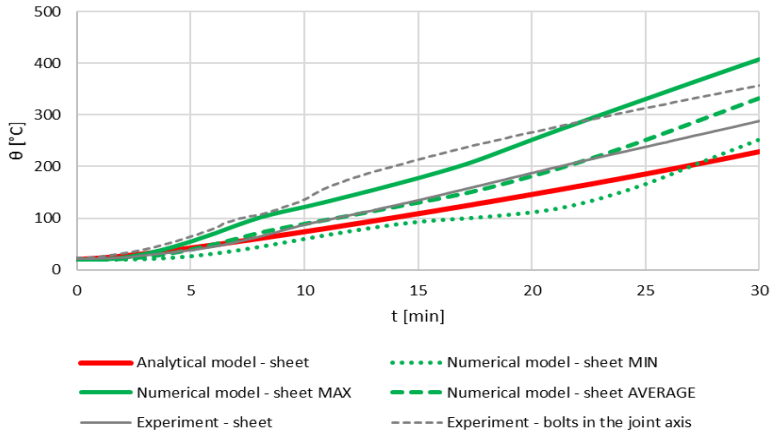


*Fig. 8: Comparison of steel sheet temperatures.*

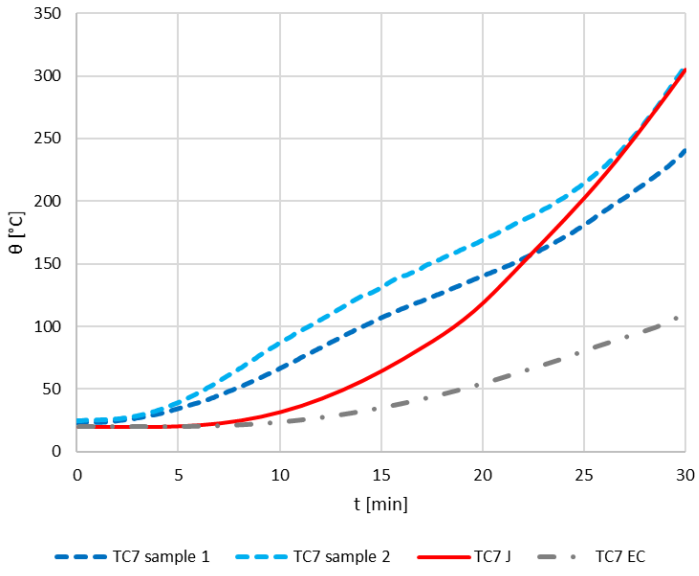

*Fig. 9: Comparison of timber temperatures of thermocouple TC7.*

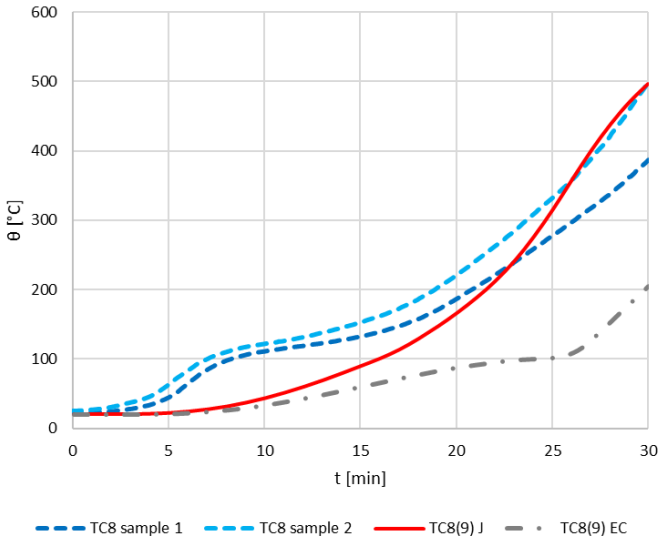


*Fig. 10: Comparison of timber temperatures of thermocouple TC8.*

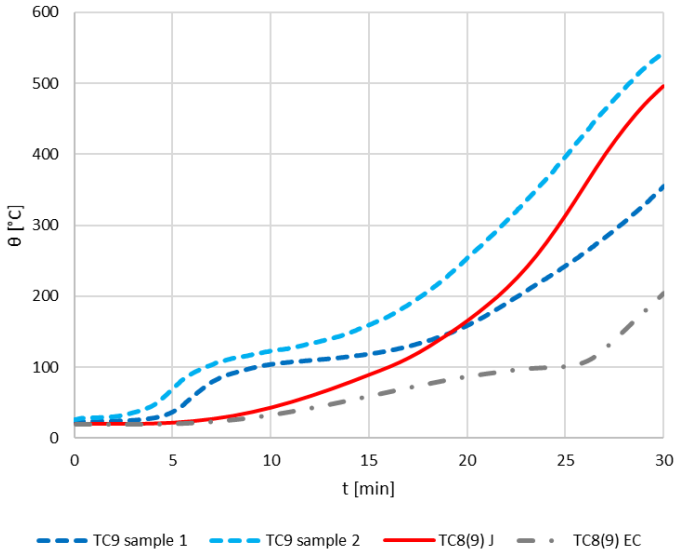


*Fig. 11: Comparison of timber temperatures of thermocouple TC9.*

## CONCLUSIONS

The paper presents a numerical model of a timber joint with an inserted steel plate under fire exposure. The model as well as experimental programme conducted for validation of the model is focused on heat transport in the joint, which is affected by the presence of the steel plate and bolts.

In order to investigate the heat transfer in the bolted steel-timber joint, the numerical model built in the Ansys software was created. The model takes into account the material properties depending on the temperature and accumulated water vapour and its condensation at the sheet by modifying of the specific heat capacity of wood in a thickness of 3 mm at the steel plate.

The simulated joint is exposed to temperature following standard temperature time curve for 30 min.

To validate the numerical model, two fire tests of the steel-timber joint were carried out in the middle-sized furnace. Temperatures measured in several positions of steel sheet, bolts and timber elements then serve for model validation. The results show that calculated temperature of bolts inside the timber and average temperature of the steel sheet correspond well with experimental measurement. Considering temperatures in timber, the model with timber properties taken from Janssens (1993) correlate better with experimental values. A local adjustment of specific heat capacity of wood which simulate the presence of accumulated water vapour and its condensation at the sheet delays the calculated temperatures compared to the experimental temperatures. The thickness of the modified wood layer was set to a value of 3 mm (Audebert et al. 2014). To refine the model, it would be appropriate to perform a sensitivity study of the effect of adjusted wood layer thickness on resulting temperatures inside the timber joint. In the frame of validation, thickness of a residual cross-section was also analyzed. Residual cross-section calculated between bolts is in good agreement with experimental results.

The results of validated numerical model were also compared to the analytical model. The analytical model is based on principles of design at normal temperatures with reduced material properties of individual components. The properties of the steel element are reduced according to Eurocode 3 and wooden according to Eurocode 5. Comparing to numerical model the analytical model gives higher temperature of bolt and lower temperature of steel sheet. For temperature of bolts inside the timber the analytical model may be assumed as safe. On the other side, it is at unsafe side for steel sheet which is inserted into timber joint. Considering the thickness of the residual cross-section the analytical model gives higher values comparing to the numerical model.

Despite the fact a number of simplifications were introduced into the model, such as omitting water vapour transport and exothermic reactions in the burning timber, temperature calculated in the numerical model corresponds well to measured values. The temperature deviation is in the range of 50°C. To reach the most accurate results of temperature profile in the bolted steel-timber joint authors recommend to use Janssen´s properties of wood with the combination of a local adjustment of specific heat capacity of wood which simulate the presence of accumulated water vapour and its condensation at the sheet.

## ACKNOWLEDGMENTS

The authors would like to thank for the financial support provided by The Czech Science Foundation (GACR) through Project No. 19-22435S. A part of numerical modelling was supported by the CTU grant for Ph.D. students SGS19/150/OHK1/3T/11.

## REFERENCES


1. Audebert, M., Dhima, D., Taazount, M., Bouchair, A., 2011: Numerical investigations on the thermo-mechanical behavior of steel-to-timber joints exposed to fire. Engineering Structures 33(12): 3257-3268.
2. Audebert, M., Dhima, D., Taazount, M., Bouchair, A., 2012: Behavior of dowelled and bolted steel-to-timber connections exposed to fire. Engineering Structures 39: 116-125.
3. Audebert, M., Dhima, D., Taazount, M., Bouchair, A., 2014: Experimental and numerical analysis of timber connections in tension perpendicular to grain in fire. Fire Safety Journal 63: 125-137.
4. Buchanan, A.H., 2001: Structural design for fire safety. John Wiley & Sons, Chichester, UK, 440 pp.
5. Cábová, K., Hasalová, L., Apeltauer, T., Kučera, P., Wald, F., 2019: Ověřování modelů v požární bezpečnosti (Model validation in fire safety). Czech Technical University in Prague, 199 pp.
6. EN 1991-1-2, 2003: Eurocode 1. Actions on structures. Part 1–2: General actions. Actions on structures exposed to fire.
7. EN 1993-1-2, 2005: Eurocode 3. Design of steel structures. Part 1–2: General rules. Structural fire design.
8. EN 1995-1-1, 2004: Eurocode 5. Design of timber structures. Part 1-1: General. Common rules and rules for buildings.
9. EN 1995-1-2, 2004: Eurocode 5. Design of timber structures. Part 1–2: General rules. Structural fire design.
10. EN 338, 2016: Structural timber. Strength classes.
11. Frangi, A., Erchinger C., Fontana M., Bouchaïr A., 2009: Experimental fire analysis of steel-to-timber connections using dowels and nails. Fire and Materials 33(12): 580-589.
12. Hassanieh, A., Valipour, H.R., Bradford, M.A., Sandhaas, C., 2017: Modelling of steel-timber composite connections: Validation of finite element model and parametric study. Engineering Structures 138: 35-49.
13. ISO 834-1, 1999: Fire- resistance tests. Elements of building construction. Part 1: General requirements.
14. Janssens, M., 1994: Thermo-physical properties for wood pyrolysis models. Pacific Timber Engineering Conference Gold Coast, Australia. Pp 607-618.
15. Johansen, K., 1949: Theory of timber connections. International association for bridge and structural engineering (IABSE). Pub. 9: 249–622.
16. Kharouf, N., Mcclure, G., Smith, I., 2003: Elasto-plastic modeling of wood bolted connections. Computers & Structures 81(8-11): 747-754.
17. Palma, P., Frangi, A., 2019: Modelling the fire resistance of steel-to-timber dowelled connections loaded perpendicularly to the grain. Fire Safety Journal 107: 54-74.
18. Palma, P., Frangi, A., Hugi, E., Cachim, P., Cruz, H., 2014: Fire resistance tests on beam-to-column shear connections. In: 8th International Conference on Structures in Fire (SiF`14), Shanghai, China. Pp 545-555.

19. Schmidt, J., Kaliske, M., 2009: Models for numerical failure analysis of wooden structures. Engineering Structures 31(2): 571-579.
20. Simões da Silva, L., Santiago, A., Vila Real, P., 2001: A component model for the behaviour of steel joints at elevated temperatures. Journal of Constructional Steel Research 57(11): 1169-1195.
21. Xu, B.H., Taazount, M., Bouchair, A., Racher, P., 2009: Numerical 3D finite element modelling and experimental tests for dowel-type timber joints. Construction and Building Materials 23(9): 3043-3052.
22. Vopatová, K., Cábová, K., Židlický, B., Kuříková, M., 2019: Advanced design of joints with steel elements in timber structures. In: Engineering Mechanics 2019: Book of full texts. Prague: Institute of Thermomechanics, AS CR. Pp 395-398.
23. Vopatová, K., Cábová, K., Židlický, B., Kuříková, M., Wald F., 2021a: Advanced design of steel to timber bolted joints. Eurosteel, Sheffield. Pp 886-891.
24. Vopatová, K., Zeman, J., Cábová, K., 2021b: Modelling of steel to timber joint exposed to fire. Proceedings of International Conference in Ljubljana, Applications of Structural Fire Engineering. Pp 367-372.
25. Zeman, J., 2021: Modelling of steel to timber joint of timber structures exposed to fire. Diploma Thesis, Czech technical university in Prague (in Czech), 81 pp.

KRISTÝNA VOPATOVÁ*, KAMILA CÁBOVÁ
CZECH TECHNICAL UNIVERSITY IN PRAGUE
FACULTY OF CIVIL ENGINEERING
THÁKUROVA 2077/7
166 29 PRAGUE 6
CZECH REPUBLIC
*Corresponding author: kristyna.vopatova@fsv.cvut.cz